

VSI: TECHNART 2025

# Unravelling the link between the *simulacra* of St Clemente of Palácio Nacional de Queluz and St Fortunato & St Semuc of Santa Casa da Misericórdia de Almada



Teresa Ferreira<sup>a,b,\*</sup>, Margarida Nunes<sup>a,c,\*</sup>, Ana Curto<sup>a</sup>, Ana Manhita<sup>a</sup>, Joana Palmeirão<sup>a,d</sup>, Luís Piorro<sup>e</sup>

<sup>a</sup> Universidade de Évora, HERCULES Laboratory/IN2PAST, Évora, Portugal

<sup>b</sup> Universidade de Évora, Escola de Ciências e Tecnologia, Departamento de Química e Bioquímica, Portugal

<sup>c</sup> University of the Basque Country, Department of Analytical Chemistry, Faculty of Pharmacy, Vitoria-Gasteiz, Spain

<sup>d</sup> Universidade Católica Portuguesa, CITAR, School of Arts, Porto, Portugal

<sup>e</sup> Museus e Monumentos de Portugal, Laboratório José de Figueiredo, Lisboa, Portugal

## ARTICLE INFO

### Article history:

Received 23 December 2025

Accepted 12 June 2026

### Keywords:

Relics

Radiocarbon dating

Textile analysis

Image-based morphometric analysis

Religious heritage

## ABSTRACT

This work presents a comparative osteological, material, and technical investigation of three 18th-century *simulacra* preserved in Portugal, aiming to clarify their origin, circulation, assembly, and shared workshop practices. Archival documentation and authentication seals confirmed their Roman origin and circulation during the 1770s. Radiocarbon dating places the skeletal remains between the 3rd and 5th centuries, spanning both periods of Christian persecution and subsequent imperial consolidation. Osteological, radiographic, and endoscopic analyses revealed differing anatomical configurations: St Semuc and St Fortunato incorporate remains from multiple non-adult individuals, assembled through deliberate substitution and consolidation practices, whereas St Clemente preserves a largely complete and anatomically coherent skeleton of a probable young adult male. Nevertheless, a similar assemblage for the body was uncovered for all *simulacra*. Facial modelling relied on silk gauze tiers, stiffened with various organic materials, alone or mixed, including proteinaceous and resin binders, such as collagen-based glues and conifer colophony-type. Imaging-based morphometric analysis was used to explore the weave type, and similar morphometric parameters were estimated, indicating a deliberate and coherent choice of gauze type. Ultimately, SEM-EDS showed that "false gold" strips (gilt-silvered-copper strips) were used in the *simulacra*'s helmets. Overall, the interdisciplinary approach evidenced that *simulacra* were assembled as devotional reliquaries likely in Rome, and that they shared the same workshop or similar workshop practices.

© 2026 The Author(s). Published by Elsevier Masson SAS. This is an open access article under the CC BY license (<http://creativecommons.org/licenses/by/4.0/>)

## 1. Introduction and research aims

### 1.1. The emergence and dissemination of the *simulacra*

The rediscovery of the Roman catacombs (1578) along the Via Salaria reshaped Catholic devotional practices. These subterranean galleries, interpreted as burial grounds of early Christians martyred under Roman persecution, became a source of *corpi santi* (full-body skeletal remains considered relics by the Catholic Church) whose exhumation, authentication, and circulation soon extended across Catholic Europe.

By the late 17th century, the simple wooden boxes housing the *corpi santi* had evolved into elaborated *simulacra*: human-shaped reliquaries in which bones were anatomically articulated, supported by internal metal structures, clad in sumptuous garments, and exhibited in glass-fronted urns. Over the following two centuries, *simulacra*'s manufacturing evolved stylistically, particularly in bodily postures and facial modelling. The *simulacra* in Portugal can be classified into three typologies, each with distinctive body positioning and standardised material for the face and limbs. During the last half of the 18th century, particularly in the 1770s, many *simulacra* exhibit a laterally reclined body, with an arm bent or aligned along the torso and the head resting on the arm or cushions, conforming to the second typology [1]. Additionally, textiles with similar patterning are used in different garments, providing key insights for their classification into the second typology. In Por-

\* Corresponding authors at: Universidade de Évora, HERCULES Laboratory/IN2PAST, Évora, Portugal.

E-mail addresses: [tasf@uevora.pt](mailto:tasf@uevora.pt) (T. Ferreira), [mrmnp@uevora.pt](mailto:mrmnp@uevora.pt) (M. Nunes).

tugal, several examples share these compositional and morphological characteristics, reflecting the repetition of models and assembly practices, i.e. shared *modus operandi*. This consistency has raised the question of whether dedicated workshops, possibly based in Rome, were responsible for producing *simulacra* that were then sent worldwide.

### 1.2. Three simulacra in Portugal as a lens for workshop practices

Within this context, the *simulacra* of St Semuc, St Fortunato, and St Clemente offer a singular opportunity to examine workshop practices from a material and technical perspective. St Semuc and St Fortunato are preserved at the Santa Casa da Misericórdia de Almada (SCMA), while St Clemente is held by the National Palace of Queluz (NPQ). They exhibit consistent characteristics that align with other 1770s examples. Authentication seals affixed to the top and back of their urns constitute documentary evidence of their circulation during this period, while no records of commission or transport were found until now. Consequently, their study relies primarily on the interpretation of materials and their technical production.

Although research on *simulacra* has expanded recently, it has focused predominantly on historical-artistic aspects. Only a handful of studies have integrated systematic analytical examination with archival research, leaving significant gaps in the question raised before: how these artefacts were manufactured and by whom, how distinct workshops operated, and how materials were selected and combined. Notable examples include the work of Sánchez Reyes [2] on Mexican *simulacra* and Pfeiffer [3] on German examples, integrating technical data and contextual evidence, to elucidate assembly characteristics of local *simulacra*. In Portugal, early contributions by Palmeirão [3] and subsequent advances within the Holy Bodies project [4], including a detailed study of two child *simulacra* [5], opened critical paths. Their fragile condition offered unique access, so their assembly was exhaustively documented. Nevertheless, a broader comparative technical framework is still missing.

### 1.3. Research aims and contribution

This study presents a comparative material and technical investigation of three Portuguese *simulacra* with three main goals: i) to shed light on their origin, circulation, and arrival in the country, through archival evidence and radiocarbon dating; ii) to elucidate assembly techniques and compare textiles; iii) to assess whether they reflect shared workshop practices and material choices. Particular attention is given to material features that may serve as diagnostic markers of workshop identity, including skeletal configuration, garments, and metal-threaded helmets. To address these aspects, a interdisciplinary approach was adopted, integrating archival research with material characterisation. Archival sources were examined to uncover the origin and historical context of the *simulacra*. Visual inspection and digital microscopy enabled detailed documentation of posture, textile morphology, and conservation state. In situ digital radiography and endoscopy revealed the internal metal structure supporting the skeletal remains, together with the surrounding hexagonal metal mesh that encloses and shapes the body. Chronological data were obtained by radiocarbon dating, while chromatographic analyses (Py-GC/MS) and FT-IR spectroscopy provided insights into binders and fibres. The composition and manufacturing technology of metal threads were estimated using SEM-EDS.

Situating these *simulacra* within broader European material and technological trends provides new evidence on how manufacturing strategies, prioritised materials, and technical decisions may reflect workshop identity, economic constraints, and aesthetic preferences.

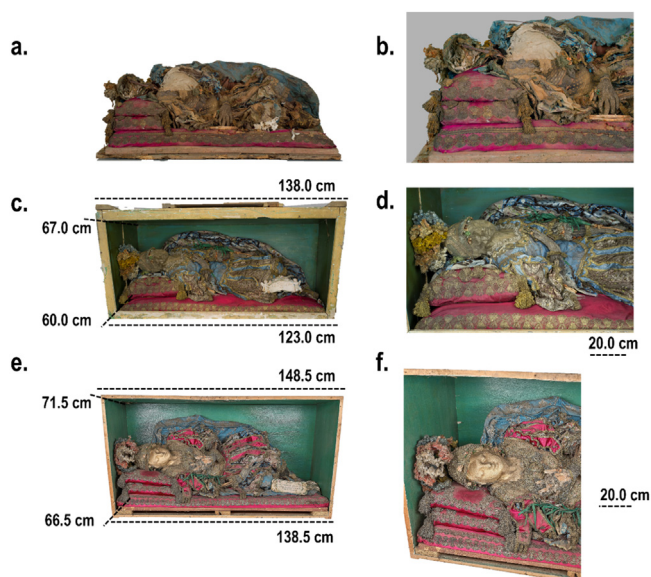


Fig. 1. *Simulacra*: a,b) St Semuc, c,d) St Fortunato, and e,f) St Clemente, with the urns' dimensions.

Overall, this work lays the foundation for future cross-regional comparisons across Europe.

## 2. Material and methods

Limited sampling was conducted in the fragile areas of *simulacra* (e.g., loose skeletal fragments, lacunae, detached or loose metal threads), in a total of 30 samples, detailed in the Supplementary Material (SM) (Table SM.1). The analytical approach conducted in this work included digital documentation and analytical characterisation (OM, SEM-EDS, ATR-FT-IR,  $\mu$ -Raman, TGA, Py-GC/MS), radiocarbon dating and image-based morphometric analysis for the estimation of gauze morphometric parameters using ImageJ® (SM, Section 2). Osteometric measurements were obtained using a sliding calliper and a measuring ruler. Sex estimation was performed using metric analysis of the radial head [6]. Age estimation of non-adult individuals was conducted through long bone length measurements [7], the assessment of developmental stages [8], and dental development and eruption patterns [9].

## 3. Results and discussion

### 3.1. The simulacra - current conservation condition and historical development & origin

Fig. 1 illustrates St Semuc and St Fortunato (SCMA) and St Clemente (NPQ). The three *simulacra* conform to the second typology defined in Palmeirão's classification system [1]. From a stylistic point of view, fundamental similarities can be found in the masks' facial features, the helmets, and the textiles used in their garments, despite these elements appearing to have been swapped between different outfits. Together, these aspects suggest a possible common workshop context for their assembly. Additional details are supplied in the SM (Fig. SM.2).

The *simulacra* exhibit different conservation states. St Semuc is in the most critical condition, with loose skeletal remains, torn and detached garments, and a severely weakened overall structure. Clear evidence of rodent activity has further compromised its integrity. In contrast, St Fortunato and St Clemente are comparatively better preserved, though they also exhibit notable signs of degradation. Both show decay in their garments, including loss of

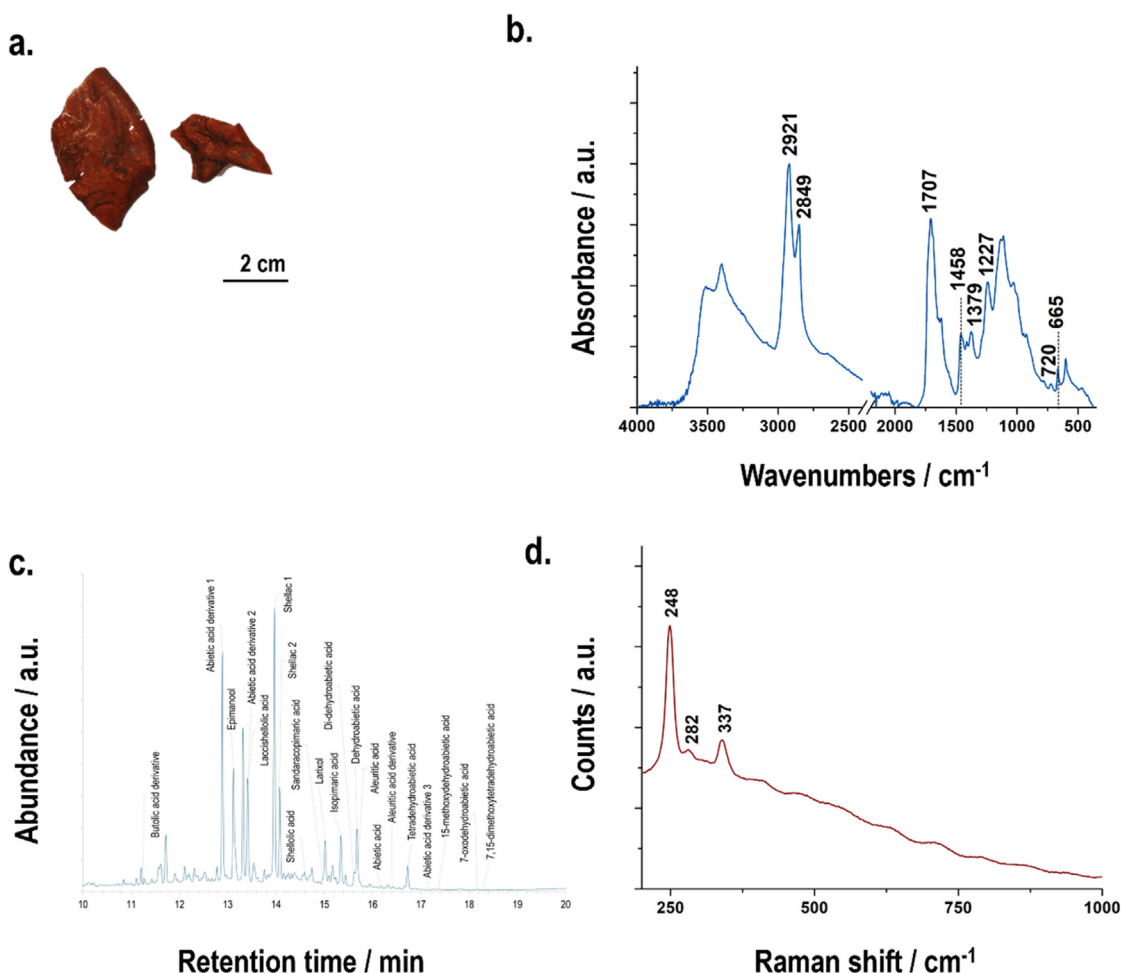


**Fig. 2.** a) 3D digital microscopic image (Clm12); b) FT-IR spectrum (Clm12); c) Pyrogram (F1); d)  $\mu$ -Raman spectrum (Clm12), highlighting the features discussed in the main text.

cohesion and integrity, soiling, staining, and fading. Localised damage caused by rodent activity has affected St Clemente's hands and feet (SM, Fig. SM.3).

In the storage building of St Bárbara's estate, where the SCMA *simulacra* were previously stored before this study, the urn of St Semuc had been placed directly on the floor, surrounded by accumulated debris, which strongly contributed to its current critical condition. In contrast, the urn of St Fortunato was placed above the ground level, resulting in a less severe state of conservation, while St Clemente's urn remained unknown, kept inside a locked wooden altar in the NPQ. The *simulacrum* was discovered during conservation works carried out in the Palace chapel (SM, Fig. SM.4).

Inside the urns, paper cartouches presented Latin inscriptions providing limited yet valuable information (Fig. SM.5): St Fortunato's describes him as a young adult, while St Clemente's explicitly records provenance from the Catacombs of St Laurence in Rome. St Semuc's cartouche was severely damaged by rodents, rendering the inscription unreadable. Nevertheless, archival records from the Misericórdia de Almada [10] indicate that the skeletal remains of St Semuc and St Fortunato originated from the Catacombs of St Callixtus (Rome) (Fig. SM.6). Although the documentary evidence concerning their arrival in Portugal is scarce, it was possible to outline some trajectory. This information is supplied in the SM (Fig. SM.7 and preceding text).

Key information on the arrival of the *simulacra* in Portugal was uncovered on the urns. Red seals were found placed side by side on a textile ribbon crossing the top, and the back of the urns

(Figs. 2a and SM.8). The seals of St Semuc and St Clemente were clearly identifiable, while the seal of St Fortunato was more challenging to read due to accumulated dust and degradation. A comparison with previously documented seal imprints from child *simulacra* [5] allowed for the identification of the coat of arms of Nicola Landini, Titular Bishop of Porphyreon (1764–1782) and Prefect of the Sacred Apostolic Church. This identification was crucial, as it confirmed that the authentication and shipment of the three *simulacra* occurred during Landini's period of activity, thereby supporting the previously discussed chronological window during which such relics were circulating from Rome.

Loose fragments of the seals (S40, from St Semuc's urn; F1, St Fortunato's; and Clm12, St Clemente's) were collected and analysed using ATR-FT-IR, Py-GC/MS, and  $\mu$ -Raman. Identical spectra and chromatographic profiles were obtained for all samples. Bands at 2921 and 2849  $\text{cm}^{-1}$ ,  $\nu_{\text{as}}\text{CH}_2$  and  $\nu_{\text{s}}\text{CH}_2$ , respectively; 1707  $\text{cm}^{-1}$ ,  $\nu_{\text{s}}\text{C}=\text{O}$ ; 1458  $\text{cm}^{-1}$ , scissoring  $\text{CH}_2$ ; 1379  $\text{cm}^{-1}$ ,  $\delta\text{CH}_3$ ; 1227  $\text{cm}^{-1}$ ,  $\nu\text{CO}$ ; 720  $\text{cm}^{-1}$ , rocking  $\text{CH}_2$ ; 665  $\text{cm}^{-1}$ ,  $\delta\text{CCC}$  [11] dominated the FT-IR spectrum, suggesting that resins were used for seal's production (Fig. 2b). Moreover, Py-GC/MS (Fig. 2c) identified derivatives of abietane and pimarane acids, along with labdane-type alcohols such as epimanol and larixol, a characteristic biomarker of Venice turpentine resin [12,13]. Shellac resin was also identified, following the detection of sesquiterpenoid acids, including laccishellolic and shellolic acids, as well as aleuritic acid and a derivative of butolic acid. Additionally, a series of short-chain fatty acids arising from the fragmentation of aleuritic acid was observed [13,14]. The use

**Table 1**  
TGA results for the silk samples (Fig. SM.9c-e).

	sample		
	Clm14	F44	S50
Moisture content (%) (33 °C < T < 120 °C)	3.1	3.3	3.6
Main mass loss (%) (200 °C < T < 450 °C)	38.3	38.7	43.3
Onset T for thermal degradation (°C)	298	294	292
T for the fastest thermal degradation (°C)	324	314	314
Residual char (%)	42.6	44.5	39.2

of calcium sulfate as a hardening agent was also identified through FT-IR with bands at 3521  $\text{cm}^{-1}$ ,  $\nu\text{OH}$ ; 1128  $\text{cm}^{-1}$ ,  $\nu_{\text{as}}\text{SO}_4^{2-}$  ( $\nu_3$  mode); 603  $\text{cm}^{-1}$ ,  $\nu_{\text{as}}\text{SO}_4^{2-}$  ( $\nu_4$  mode).  $\mu$ -Raman analysis showed that the red pigment used to colour the seals was vermilion (HgS) (Fig. 2d), with Raman symmetric stretching  $A_1$  mode (248  $\text{cm}^{-1}$ ) and two degenerated E modes, longitudinal ( $E_{\text{LO}}$ , 282  $\text{cm}^{-1}$ ) and transverse ( $E_{\text{TO}}$ , 337  $\text{cm}^{-1}$ ) characteristics of this pigment [15].

The textile ribbons running around the urns (S50 from St Semuc's, F44 from St Fortunato's, and Clm14 from St Clemente's) featured yellowish warp threads and predominantly light-green weft (Fig. SM.9a), with all ribbons measuring 2 cm wide. Dark-field microscopy (Fig. SM.9b), together with FT-IR analysis (Fig. 3c), confirmed the silk (animal) origin of the textile fibres. Considering that the urns of St Semuc and St Fortunato arrived in Portugal together, and that the urn of St Clemente most likely arrived during the same decade, we hypothesise that the silk used in the three ribbons may have originated from the same supplier. TGA analysis was employed to evaluate the moisture content and thermal stability of the silk weft, while FT-IR analysis provided complementary information on the degree of material degradation. Silk fibres primarily consist of proteins fibroin and sericin, with the latter mainly removed with associated impurities from the silk thread during textile manufacturing.

All samples exhibit a minor initial mass loss between 30 and 120 °C upon heating, attributable to the loss of adsorbed moisture. The dominant degradation stage occurs between ~250 °C and 350 °C and ends around 450 °C, as evidenced by a sharp peak in the DTG curves (Fig. 3b). Beyond this step, continuous mass loss is observed up to 750–800 °C, leaving a significant residual char (Fig. 3a). This thermal behaviour is consistent with that reported for native silks at 10 °C/min under a  $\text{N}_2$  atmosphere [16]. Detailed TGA profiles, including mass losses, onset T, and other parameters, are illustrated in Fig. SM.9c-e, with a summary of the results presented in Table 1. Briefly, Clm14 is the best preserved and exhibits the highest thermal stability among the wefts. F44, although seeming less thermally robust, remains in good condition, while S50 shows the highest level of degradation. Further discussion is detailed in SM (Fig. SM.9 and thereafter).

FT-IR spectroscopy provided insights into the molecular alteration of the silk ribbons. A detailed band assignment is reported in Table SM.2. Overall, only minor shifts in band position and intensity were observed. An intensity ratio-based approach [17] was adopted to estimate three degradation indices for fibroin: (i) the Amide I crystallinity index ( $A_{1619}/A_{1699}$ ), reflecting the relative proportion of parallel to antiparallel  $\beta$ -sheets; (ii) the Amide III crystallinity index ( $A_{1260}/A_{1229}$ ), which informs on the ratio of antiparallel  $\beta$ -sheets strands to random coil content, and (iii) the AmideI/AmideII ratio ( $A_{1619}/A_{1509}$ ), indicative of oxidation-related alterations affecting the primary structure of fibroin.

The Amide I and Amide III crystallinity indices present contrasting trends. In the ( $A_{1619}/A_{1699}$ ) index, S50 shows the lowest ratio (3.51), whereas Clm14 and F44 had higher, nearly identical values (4.46 and 4.31, respectively). The lower value for S50 re-

flects the decrease of the parallel  $\beta$ -sheets (presumably less stable) in favour of the antiparallel  $\beta$ -sheets (more stable) in the crystalline region of the polypeptide [17,18]. In addition, in the Amide III region, S50 showed the highest  $A_{1264}/A_{1230}$  ratio (0.91) among Clm14 (0.85) and F44 (0.88), pointing out an increase in the crystalline antiparallel  $\beta$ -sheet structure with respect to random-coil content, more disordered regions that seem to undergo faster degradation, as was already observed for cellulose [17,19]. These insights imply that degradation may preferentially target less stable regions of the fibroin matrix, likely promoting chain scission and rearrangement before recrystallisation, thereby increasing antiparallel  $\beta$ -sheet content. Changes in the carbonyl region further support this interpretation. Notably, S50 is the only sample presenting a broad shoulder at 1733  $\text{cm}^{-1}$  ( $\nu\text{C=O}$ ), likely associated with ageing-induced processes, primarily oxidation [18]. Nevertheless, the negligible differences in the ( $A_{1619}/A_{1509}$ ) ratio suggest that hydrolytic processes may play a more significant role than oxidation in this case. The presence of water is known to promote peptide-bond cleavage, form COOH- groups, and affect the crystalline organisation of silk fibroin [19]. Consequently, the prolonged exposure to fluctuating humidity and high temperatures in the floor of St Barbara's storage building may have contributed to the behaviour of the S50 sample.

The apparent discrepancy between the higher fraction of antiparallel  $\beta$ -sheet structure and the lower thermal stability observed in TGA results for sample S50 arises because  $\beta$ -sheet crystallinity reflects local secondary structure. In contrast, the least stable molecular domains govern thermal degradation. This behaviour seems to reflect degradation-induced chain scission, promoting recrystallisation into thermodynamically favoured antiparallel  $\beta$ -sheets while reducing overall thermal stability.

### 3.2. Osteological analysis and skeletal assembly

The osteological study revealed differences in the anatomical assemblages of St Semuc, St Fortunato, and St Clemente.

#### • St Semuc

Radiographic examination of St Semuc showed a heterogeneous and incomplete assemblage, comprising skeletal remains from various individuals: one adult and more than one non-adult (Fig. 4a). The cranial calotte was preserved, whereas the facial bones were absent, possibly due to pre-assemblage damage and loss. Even though only limited skeletal remains were visible, this apparent absence may be attributable to the reduced radiodensity of the bones, particularly those of non-adult individuals. The left upper limb comprises a non-adult humerus and ulna. On the other hand, the radius exhibits adult morphological characteristics, consistent with those of the right upper limb, suggesting that both may belong to the same adult individual. The right radius has a maximum head diameter (24.50 mm), suggesting a male individual (considering 21.43 mm of sectioning point, and a classification rate of 89.26) [6]. The presence of a right tibia (270.00 mm) in the lower limbs, along with a left ulna (185.00 mm) in the arm, corresponds to an estimated age-at-death of 9–10 years [7]. Only three bones visible from the exterior could be measured using a calliper or a ruler. Most skeletal elements were accessible solely through the endoscope, which did not allow metric recording because it lacked an integrated scale. Non-adult metatarsals and phalanges at different developmental stages [8] were identified in the feet and the right hand by direct observation through the interstices of the openwork structure of the lace-like metal mesh sandals and gloves, confirming the presence of remains from multiple individuals. Radiocarbon dating of a non-adult bone fragment (S42) produced an age of 1711  $\pm$  30 BP (years before present). Calibration using OxCal v4.4 [20] and the IntCal20 calibration curve,

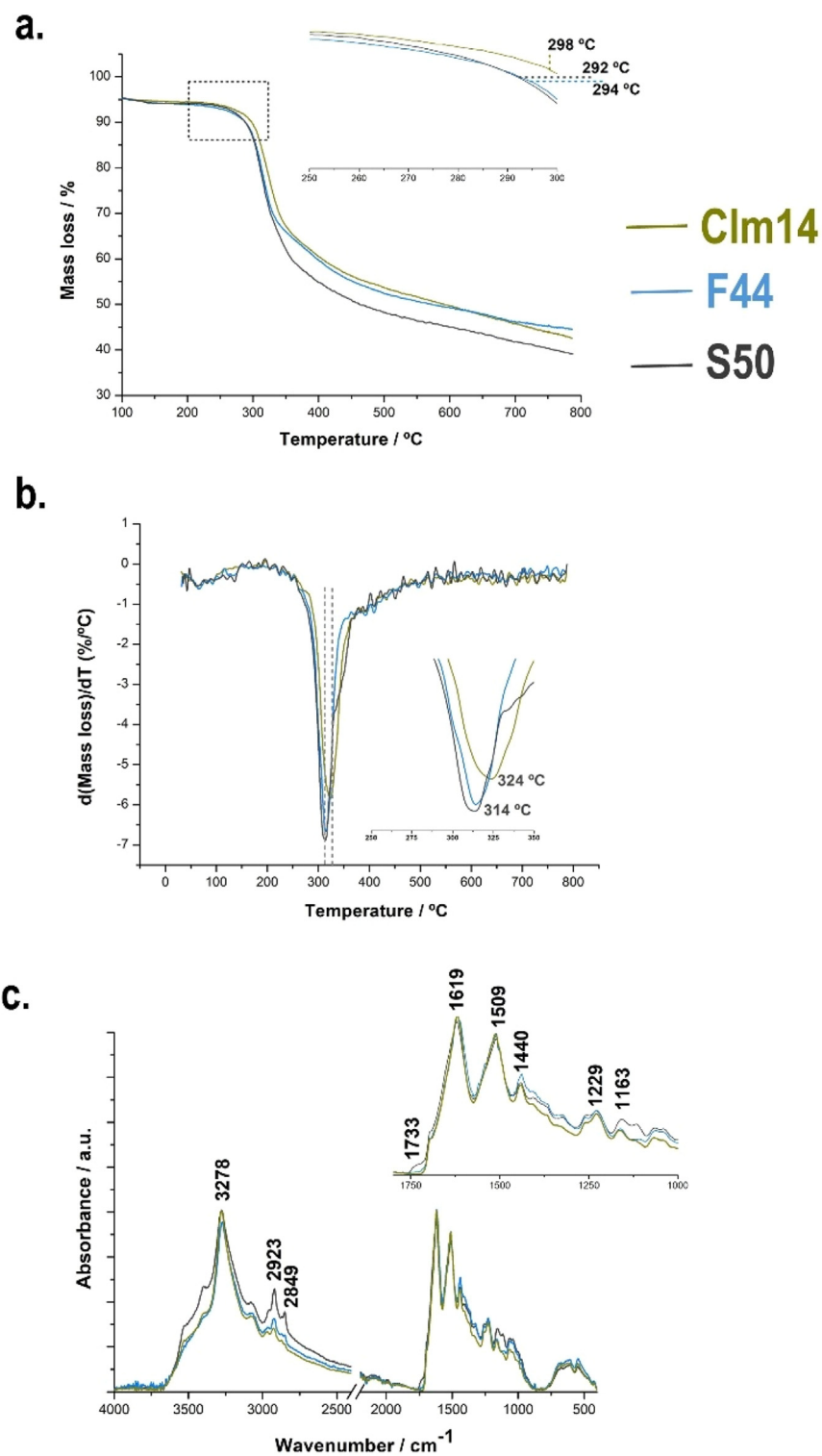


**Fig. 3.** Samples Clm14, F44, and S50: a) Overlay of the TGA profiles from 30 to 800 °C for direct comparison; b) derivative of percentage mass loss as a function of temperature (DTG curves); c) FT-IR spectra showing characteristic features of the silk fibre.

at a  $2\sigma$  confidence level (95.4%), yielded a calibrated age range of cal AD 250–410 (calibrated Anno Domini (cal AD)) (Fig. SM. 10). Within this range, the highest probability intervals were cal AD 250–295 (28.3%) and cal AD 311–410 (67.1%). This data places the remains in a transitional period in early Christian history, from the end of the Great Persecution (303–311 AD) to the consolidation of Christianity as the official religion of the Roman Empire

(380 AD). While coinciding with the final episodes of anti-Christian violence under Diocletian, this timeframe follows the Edicts of Toleration (311 AD) and Milan (313 AD), which ended Christian persecution. Under Constantine (324–337 AD) and subsequently Theodosius I (379–395 AD), Christianity gained imperial favor and became the state religion, making any later martyrdom highly unlikely.

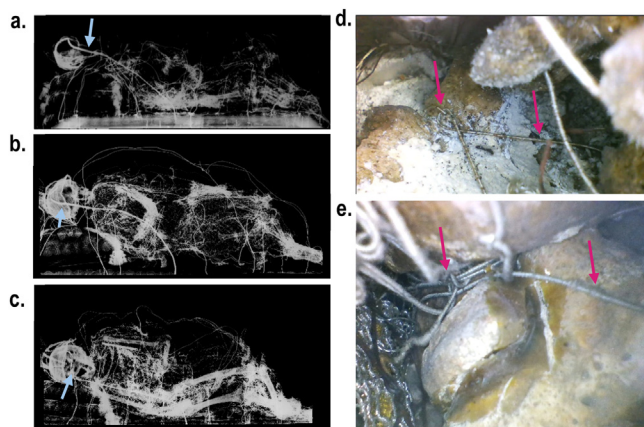


**Fig. 4.** Radiographic images of a) St Semuc, b) St Fortunato, and c) St Clemente, with blue arrows indicating the central metal cable holding the skull. Endoscope images showing the d) *os coxae* St Semuc, where a white consolidating substance was applied to join the unfused *ilium*, *ischium*, and *pubis* bones; e) knee of St Clemente (femur, patella, and tibia), illustrating the presence of a wax-like coating used in the bone, and thin wires (pink arrows) to secure the bones to the hexagonal metal mesh shaping the body. (For interpretation of the references to colour in this figure legend, the reader is referred to the web version of this article.)

Endoscopic examination provided additional insights, revealing that the *os coxae* had been consolidated with a white paste substance (Fig. 4d), likely applied to strengthen the physical integrity of the unfused *ilium*, *ischium*, and *pubis*, which only fuse after ca. 11 years of age [8]. Similar consolidation practices were recently reported in our previous work [5]. A substance of similar appearance was also used in St Semuc's mandible to fill an alveolar gap left by a missing tooth. Although no teeth were present, the absence of alveolar remodelling indicates *perimortem* or *post-mortem* tooth loss, suggesting a need for consolidation efforts to re-establish structural facial integrity.

- St Fortunato

In St Fortunato, only limited skeletal remains were externally visible, mainly from the forearms, lower limbs, hands, and feet. Digital radiography confirmed the presence of the cranium and mandible, as well as long bones corresponding to the upper and lower limbs. Nevertheless, ribs and vertebrae were not observed, probably due to their lower density (Fig. 4b). Endoscopic inspection was not performed due to the absence of entry points for the fiberoptic probe. This *simulacrum* exhibited a higher degree of anatomical substitution than St Semuc. The hands were reconstructed using non-adult ribs as metacarpal substitutes, while phalanges from the feet were repositioned as hand phalanges. Such anatomical arrangements indicate an intentional intervention, likely guided by aesthetic motivations. Osteometric and dental insights confirmed that the *simulacrum* integrates remains from at least two non-adult individuals. The right radius (104.80 mm) corresponds to an age-at-death of approximately 2.5–3 years, whereas the tibia (200.00 mm) indicates an age between 5.5 and 6 years [7]. Fig. 4b, which shows radiographic evidence of mandibular dental development, further refines this estimate, indicating an age of 4.5–5.6 years [9]. Although the estimated ages vary, they consistently indicate that all bones for which age could be estimated belonged to very young individuals. This information aligns with the inscription found in the paper cartouche —“Corpus S. Pueri Fortunati Martyris” — where *pueri* (Lat. *puēru-*) denotes “child” (Fig. SM.5c).

- St Clemente

Radiographic image of St Clemente showed a largely complete and anatomically coherent skeleton, comprising the cranium, vertebrae, ribs, *os coxae*, and all major limb bones (Fig. 4c). Evidence

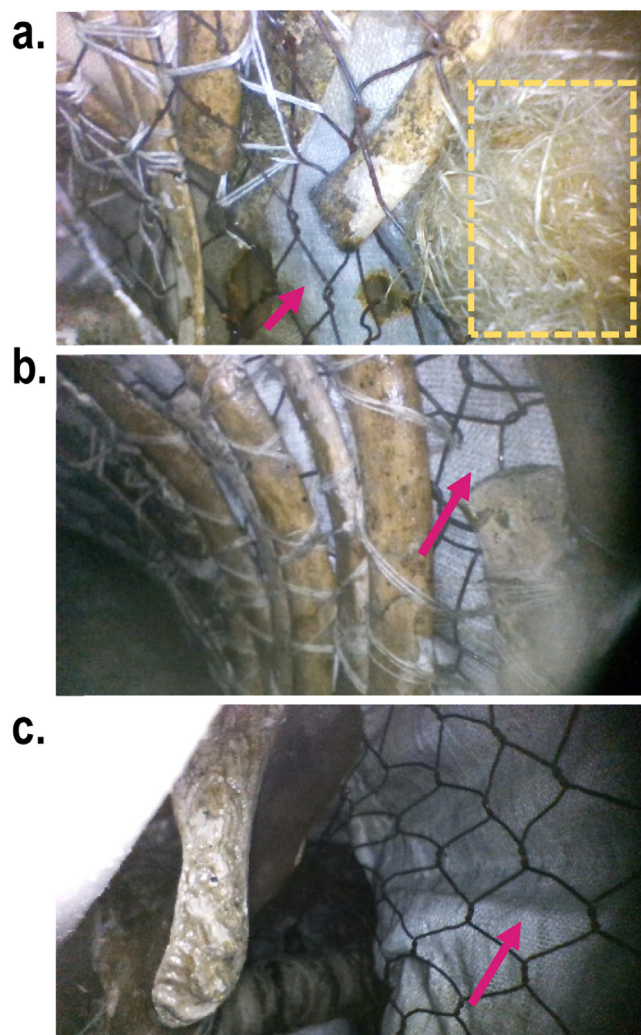


**Fig. 5.** Endoscopic images of the thoracic framework showing the hexagonal metal mesh used for the volume and anatomical positioning of the bones of: a) St Semuc; b, c) St Clemente. The ribs are sutured to the mesh, which is enveloped in a white fabric (pink arrows), shaping the bodies. Fibrous fillings are visible between the metal mesh and the fabric (yellow square). (For interpretation of the references to colour in this figure legend, the reader is referred to the web version of this article.)

of anatomical foot manipulation was observed with an incorrectly positioned metacarpal serving as a metatarsal. Additionally, a wax-like material appeared to have been applied to preserve the shape of the knee joint, particularly around the femur and patella, while on the ribs it was used as a surface coating, producing a glossy appearance (Fig. 4e and 5b). St Clemente's radiography revealed complete epiphyseal fusion of the femora and tibiae, alongside an unfused iliac crest, indicating an estimated age-at-death between 18 and 22 years [8], which is further supported by the eruption of the third molar (16–23 y.o.) [9]. The measured radius length (ca. 230 mm) indicated that the individual was likely a male [21]. These insights suggest a biological profile of a young adult male. Radiocarbon dating of a St Clemente's phalanx (C1m11) yielded the period of  $1670 \pm 30$  BP. Moreover, calibration with OxCal v4.4.4 using the IntCal20 dataset [20,22] indicates two calibrated age ranges: AD 257–282 and AD 330–436, which together account for 91.4% of probability within the 95.4% confidence range (Fig. SM.10). While the later period ranges from the end of persecutions (313 AD) of Christians to the time when Christianity was officially the religion of the Empire, the first period corresponds to a particularly difficult moment for Christian communities: Valerian (253–

**Table 2**  
Morphological characteristics of the inner and outer gauzes.

morphological characteristics	morphometric parameters	St Fortunato		St Clemente	
		inner	outer	Inner	outer
density	warp (threads/cm)	20	30	20	25
	weft (threads/cm)	20	30	25	40
	thread density ratio (warp/weft ratio)	1.0	1.0	1.0	0.6
thread diameter	warp ( $\mu\text{m}$ )	152 $\pm$ 17	73 $\pm$ 10	145 $\pm$ 22	83 $\pm$ 8
	weft ( $\mu\text{m}$ )	152 $\pm$ 27	85 $\pm$ 13	127 $\pm$ 30	83 $\pm$ 9
interstitial spacing	distance between adjacent warp threads ( $\mu\text{m}$ )	1033 $\pm$ 98	799 $\pm$ 48	1099 $\pm$ 111	795 $\pm$ 102
	distance between adjacent weft threads ( $\mu\text{m}$ )	822 $\pm$ 91	389 $\pm$ 40	745 $\pm$ 89	498 $\pm$ 33
warp crossing frequency	no. of warp crossing/cm	28 $\pm$ 4	30 $\pm$ 3	25 $\pm$ 5	30 $\pm$ 3
weave type	structural pattern	single leno		single leno	
crossing angle	crossing angle of paired warp threads ( $^\circ$ )	28.3 $\pm$ 2.7	30.1 $\pm$ 2.1	25.4 $\pm$ 2.3	29.9 $\pm$ 3.4

\*the identification of warp and weft directions was facilitated by the presence of preserved selvages in the gauze, which provided direct evidence of the warp orientation.

260 AD) initiated a severe and systematic persecution with decrees in 257 and 258, demanding sacrifices to Roman gods, that resulted in executions and exiles, and targeting clergy, senators, knights, matrons but also common people [23]. The context of the later periods for St Clemente and St Semuc raises the possibility that these remains correspond to late Roman burials, later reinterpreted within the framework of devotion, rather than being the remains of persecuted martyrs.

The three *simulacra* exhibit a metal rod that extends from the cranium to the pelvis, providing structural support (Fig. 4a-c, blue arrow). The ribs were sewn to the hexagonal metal mesh (Fig. 5) that helped define the body's shape. Thinner metal wires were employed to stabilise certain bones, as previously mentioned (Fig. 4d, e). Over this mesh, a white fabric and fibrous fillings were applied to enhance the moldability to the body (Fig. 5, pink arrows and yellow square). Notably, a similar procedure was documented in our early study [5] on St Primogenita, which also featured the seal of Bishop Landini. Only for St Clemente did the white fabric serve as the first layer over the facial bones (Clm17). OM and FT-IR analysis revealed that this fabric is plant-based (cotton), while Py-GC/MS indicated the presence of a proteinaceous binder (collagen-type glue) along with a minor, partially oxidised triacylglycerol fraction. This binder was used to adhere the fabric to the facial bones and assist in shaping the face. Accessible fillings from the glove of St Semuc (S10) and sandal of St Fortunato (F42) were analysed by Py-GC/MS, revealing that they were glued to the cardboard to support the respective bones using a proteinaceous binder. Additionally, conifer resin was added to F42 (Fig. SM.11 and subsequent text).

### 3.3. Facial gauze characterisation – composition & morphology

The face was modelled using layers of different gauzes. OM and FT-IR analysis of all samples (S56, F16, F17, Clm18, and Clm19) confirmed that these gauzes are made of silk. Representative data from samples F16 and F17 from St Fortunato are shown in Fig. SM.12. The gauze layers were stiffened to shape the facial features, likely using a mould [5].

Py-GC/MS analysis of sample F16 identified protein markers, consistent with a collagen-type glue, suggesting the primary use of a proteinaceous binder as the stiffening agent. Only traces of triglyceride residues were found, and no signatures of resin, sterol, or drying oil were detected. These findings align with the previously discussed results for the St Clemente, sample Clm17. Differently, sample S56 from St Semuc yielded conifer (Pinaceae, colophony-type) resin with a non-drying or weakly drying triacylglycerol fat, with no evidence for a proteinaceous binder or a clas-

sical drying oil. Interestingly, F52 (St Fortunato), a stripped gauze from the legs, mainly presents a proteinaceous binder associated with a conifer (Pinaceae, colophony-type) resin. Further discussion is available in the SM (Section 3.3, Py-GC/MS results).

Weaving inspection showed that the facial gauzes share a conventional leno structure (SM, section 2.4), comprising two distinct tiers, each composed of three or four layers: a more open inner tier functioning as the structural support, overlaid by a denser outer tier (Fig. SM.12a, b). Quantitative weave metrics were estimated through morphometric analysis to characterise the gauzes and establish (di)similarities among the *simulacra*. The results are summarised in Table 2, with the full dataset provided in Tables SM.3–5 and visualised in Figure SM.13. The facial gauzes from St Semuc were not assessed due to severe degradation.

The outer gauzes are of higher density, but the thread density ratio between inner and outer gauzes was frequently kept constant (1:1). The trend between the density and thread diameter was found to be similar between *simulacra*. Both warp and weft threads are considerably thicker in the inner gauzes and finer in the outer gauzes. This thinning is accompanied by an increase in thread density from  $20 \times 20$  to  $30 \times 30$  threads/cm in St Fortunato and from  $20 \times 25$  to  $25 \times 40$  threads/cm in St Clemente, resulting in a more opaque external surface. Interstitial spacing measurements corroborate this observation, revealing smaller inter-thread distances in the outer gauzes. In St Fortunato, the warp spacing decreases from  $1033 \pm 98 \mu\text{m}$  in the inner gauze to  $799 \pm 48 \mu\text{m}$  in the outer gauze, while the weft spacing decreases from  $822 \pm 91 \mu\text{m}$  to  $389 \pm 40 \mu\text{m}$ . St Clemente shows the same trend, indicating a purposeful selection of gauzes with different levels of openness, likely to balance structural support and visual concealment. No significant variation in the crossing angle of paired warp threads was observed for both *simulacra*, with values ranging from  $\sim 25^\circ$  to  $30^\circ$ , indicating similar warp-tension control during weaving and common weaving practices. Although the two *simulacra* differ in thread thickness, their morphological characteristics strongly suggest similar weaving techniques and possibly the same gauze supplier.

### 3.4. “False gold strips” as a tracer of shared craft practices

A further point of correlation between these *simulacra* lies in their helmets, which resemble saints' iconography (e.g., St Michael Archangel). The helmets' surfaces are covered with metal strips fixed to the fabric, creating a laminated surface, over which decorative gilt-metal threads and a coloured silk plume on the crest are observed (Fig. SM.14, Fig. 6a). These metal strips (S16, F38, Clm15, from St Semuc, Fortunato and Clemente, respectively) showed

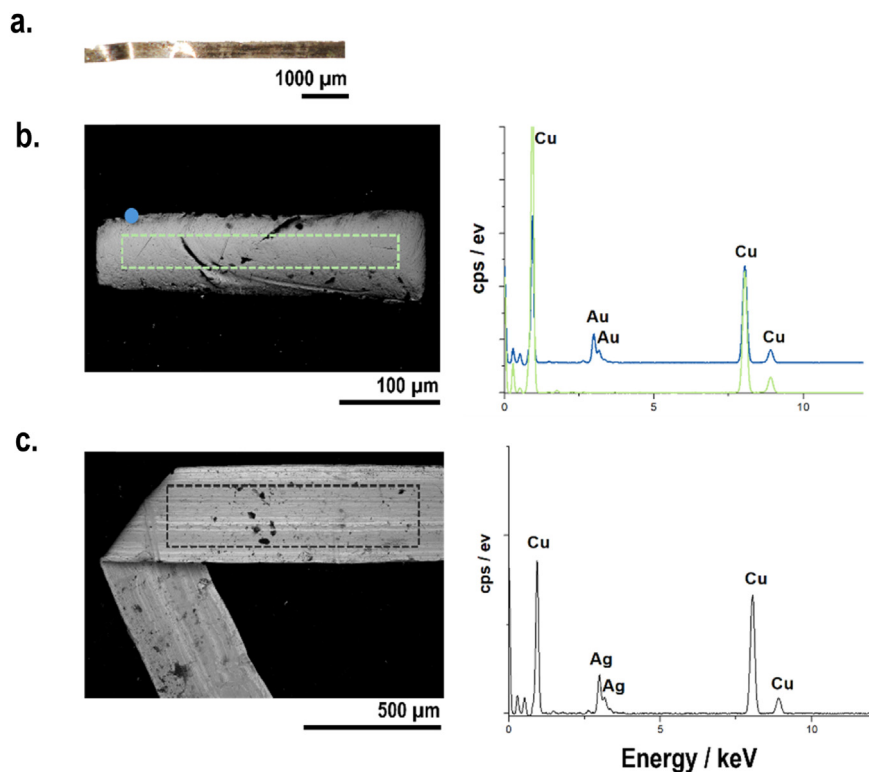


**Fig. 6.** a) OM image of St Semuc's silvery strip from the helmet (sample S16); b, c) SEM micrographs showing the strip's cross-section (with point and area analyses highlighted in blue and green) and the transversal section (analysis area highlighted in grey), with corresponding EDS spectra, respectively. (For interpretation of the references to colour in this figure legend, the reader is referred to the web version of this article.).

compositional and technological similarities. OM observations revealed a predominantly silver appearance with faint golden hues. SEM-EDS cross-sectional analysis indicated a bulk composition of Cu (100%wt) with both gilt surfaces (Fig. 6b). Additionally, longitudinal views were also analysed, revealing minor Ag amounts (2–6 wt%) (Fig. 6c). These characteristics are consistent with the so-called "false gold" [24], gilt-silvered-copper strips sparsely documented from the 17th century onward. Such metal threads were interpreted as imitations of gilt-silver threads (SM, Section 3.4). As reported by Karatzani and Jaró [24,25], gilt-silvered-copper threads were often restricted and relegated to lower-status objects or theatrical costumes. Their occurrence in historical textiles is so rare that Karatzani's [25] survey identified only four. Given that the *simulacra*'s garments were made of double-sided gilt-silver and silver threads (Table SM.6), the use of these strips in the helmets appears intentional. The purposeful selection of these materials reinforces the same workshop practices across these *simulacra*.

### 3.5. Conclusions

This study investigated the *simulacra* of St Semuc, St Fortunato, and St Clemente in Portugal, addressing their origin, circulation, assembly, and material composition, and assessing the extent to which they reflect shared workshop practices. Archival evidence and authentication seals situate the circulation of all three *simulacra* in the second half of the eighteenth century, during the episcopate of Nicola Landini (1764–1782), and confirm their Roman provenance. The seals share a consistent material composition: shellac and Vernice turpentine resins, with calcium sulfate as a hardener and vermilion as the pigment, supporting the use of standardised practices.

Importantly, radiocarbon dating of the skeletal remains placed them between the 3rd and 5th centuries. Although these ranges overlap periods of Christian persecution, they also extend into phases of Christian consolidation, rendering, in some cases, a direct identification with martyred individuals uncertain. Osteological and endoscopic images further revealed marked differences in anatomical coherence among the *simulacra*. St Semuc and St Fortunato incorporate remains from multiple non-adult individuals, with St Semuc also including adult elements, indicating a prioritisation of completeness over anatomical accuracy. Radiographic and endoscopic evidence revealed substitution practices, consolidation techniques, and bone repositioning. In contrast, St Clemente presents a complete, anatomically consistent configuration, compatible with a young adult male, with only minor manipulation. *Simulacra*'s facial modelling relied on the superposition of silk gauze tiers, stiffened with binders. Quantitative textile analysis confirmed similar morphometric parameters, indicating intentional technical choices. Overall, a similar internal metal framework, mesh-supported rib structures, and layered gauze tiers were systematically employed to shape the bodies over the skeletal remains, strongly supporting the existence of shared workshop practices, likely operating within a networked production system.

Broadly, this study underscores the interdisciplinary value of reassessing *simulacra* as composite devotional reliquaries rather than as a single container. By foregrounding materiality, assembly, and technical decision-making, it contributes to new evidence for broader discussions of the production and circulation of *simulacra* in eighteenth-century Europe, establishing a robust framework for future comparative research.

## Acknowledgements

The authors extend their heartfelt gratitude to Dr Paula Costa and the Social Bodies of SCMA for granting access to St Fortunato and St Semuc *simulacra*, archival research, and data from Costa's research, and for their full support throughout the work. We sincerely thank Dr António Nunes Pereira, Director of PNQ, and Dr Joana Loureiro from Parques de Sintra – Monte da Lua, S.A., for providing access to St Clemente during the in situ campaign. We also thank Dr Paula Monteiro for the photograph of St Clemente seals and for her support in the sampling procedures. We acknowledge Dr Rui Mendes for historical information on the relics and Prof. P. Moita for assistance with TGA analysis.

Language models (ChatGPT and Grammarly) were used to assist with refining English grammar and phrasing.

The author acknowledges FCT for funding through the Holy Bodies Project (<https://doi.org/10.54499/2022.01486.PTDC>) and J. Palmeirão's research fellowship. Ana Manhita and Ana Curto acknowledge FCT for financial support (<https://doi.org/10.54499/CEECIND/00791/2017/CP1431/CT0005> and <https://doi.org/10.54499/2020.02110.CEECIND/CP1593/CT0005>, respectively). Margarida Nunes acknowledges support from the JDC2024-053901-I grant, funded by MICIU/AEI/10.13039/501100011033 and by the ESF+. Funding was also provided through the projects <https://doi.org/10.54499/UID/PRR/04449/2025> (HERCULES Laboratory), <https://doi.org/10.54499/LA/P/0132/2020> (IN2PAST).

## Supplementary materials

Supplementary materials associated with this article can be found, in the online version, at [doi:10.1016/j.culher.2026.06.011](https://doi.org/10.1016/j.culher.2026.06.011).

## References

- [1] J. Palmeirão, *Simulacra Corporum Sanctorum Martyrum - Estudo de um Património Em Risco e Estratégias Para a Sua Valorização e Salvaguarda* PhD Thesis, Universidade Católica do Porto, 2023.
- [2] G.S. Reyes, *La Donación de Corpi Santi En México Siglos XVI – XIX, El Colegio de Michoacán*, 2021.
- [3] A.C. Pfeiffer, *Auferweckt in Herrlichkeit! Barocke Heilige Leiber in Oberschwaben: materialien* PhD Thesis, Fixierungstechniken, konservatorische Aspekte, 2005.
- [4] Holy bodies project, 2025. <https://holybodies.uevora.pt/> (Accessed date: 8 December 2025).
- [5] T. Ferreira, M. Nunes, A. Curto, J. Palmeirão, A. Manhita, F. Olival, L. Piorro, P. Monteiro, E. Vieira, The study of two impressive simulacra at Santa Casa da Misericórdia de Almada, Portugal, *Eur. Phys. J. Plus.* 140 (2025), doi:10.1140/epjp/s13360-025-06356-3.
- [6] P. Selliah, F. Martino, M. Cummaudo, L. Indra, L. Biehler-Gomez, C. Pietro Campobasso, C. Cattaneo, Sex estimation of skeletons in middle and late adulthood: reliability of pelvic morphological traits and long bone metrics on an Italian skeletal collection, *Int. J. Legal Med.* 134 (2020) 1683–1690, doi:10.1007/s00414-020-02292-2.
- [7] H. Cardoso, *Patterns of Growth and Development of the Human Skeleton and Dentition in Relation to Environmental Quality. A Biocultural Analysis of a Sample of 20th Century Portuguese Subadult Documented Skeletons*, University of Hamilton, Ontario, 2005.
- [8] M. Schaefer, S. Black, L. Scheuer, *Juvenile Osteology: a Laboratory and Field Manual*, 1st ed., Elsevier, Burlington, 2009, doi:10.1016/b978-012624000-9/50009-5.
- [9] S.J. Al Qahtani, M.P. Hector, H.M. Liversidge, Brief communication: the London atlas of human tooth development and eruption, *Am. J. Phys. Anthropol.* 142 (2010) 481–490, doi:10.1002/ajpa.21258.
- [10] A.H.S.C.M.A, PT/AHMA/SCMA/D/02/pt.06Inventário Geral da Secretaria da Santa Casa Da Misericórdia de Almada, 1948, Almada.
- [11] S. Prati, G. Sciutto, R. Mazzeo, C. Torri, D. Fabbri, Application of ATR-far-infrared spectroscopy to the analysis of natural resins, *Anal. Bioanal. Chem.* 399 (2011) 3081–3091, doi:10.1007/s00216-010-4388-y.
- [12] K.J. Van Den Berg, J.J. Boon, I. Pastorova, L.F.M. Spetter, Mass spectrometric methodology for the analysis of highly oxidized diterpenoid acids in old master paintings, *J. Mass Spectrom.* 35 (4) (2000) 512–533.
- [13] J. Mills, R. White, Basic chemistry, in: J. Mills, R. White (Eds.), *Organic Chemistry of Museum Objects*, 2nd ed., Routledge, London, 1987, pp. 0–23.
- [14] G. Chiavari, G.C. Galletti, Pyrolysis-gas chromatography/mass spectrometry of amino acids, *J. Anal. Appl. Pyrolysis* 24 (1992) 123–137, doi:10.1016/0165-2370(92)85024-F.
- [15] M. Botticelli, A. Maras, A. Candeias,  $\mu$ -Raman as a fundamental tool in the origin of natural or synthetic cinnabar: preliminary data, *J. Raman Spectrosc.* 51 (2020) 1470–1479, doi:10.1002/jrs.5733.
- [16] Y. Liu, L. Yang, C. Ma, Thermal analysis and kinetic study of native silks, *J. Therm. Anal. Calorim.* 139 (2020) 589–595, doi:10.1007/s10973-019-08420-4.
- [17] M.A. Koperska, D. Pawcenis, J. Bagniuk, M.M. Zaitz, M. Missori, T. Łojewski, J. Łojewska, Degradation markers of fibroin in silk through infrared spectroscopy, *Polym. Degrad. Stab.* 105 (2014) 185–196, doi:10.1016/j.polymdegradstab.2014.04.008.
- [18] J. Wang, J. Guan, N. Hawkins, F. Vollrath, Analysing the structure and glass transition behaviour of silks for archaeology and conservation, *J. R. Soc. Interface* 15 (2018) 20170883, doi:10.1098/rsif.2017.0883.
- [19] M.A. Koperska, J. Bagniuk, M.M. Zaitz-Olsza, K. Gassowska, D. Pawcenis, M. Sitarz, E. Bulska, J. Profic-Paczkowska, Ex situ and In situ artificial thermogravimetric study of the natural degradation of Bombyx mori silk fibroin, *Appl. Sci.* 13 (2023) 9427, doi:10.3390/app13169427.
- [20] P.J. Reimer, Composition and consequences of the IntCal20 radiocarbon calibration curve, *Quat. Res. (United States)* 96 (2020) 22–27, doi:10.1017/qua.2020.42.
- [21] P. Morandini, L. Biehler-Gomez, K. Stull, C. Cattaneo, Metric analysis of the postcranial skeleton: a comprehensive approach for biological sex estimation in an Italian population, *Int. J. Legal Med.* 140 (2025) 441–461, doi:10.1007/s00414-025-03599-8.
- [22] B. Ramsey, OxCal, OxCa from Oxford radiocarbon, accelerator unit (2021). <https://c14.arch.ox.ac.uk/oxcal.html> (Accessed 30 October 2025).
- [23] D. Wright, Christian History Institute, 313 Edict Milan, 2022. <https://christianhistoryinstitute.org/magazine/article/edict-of-milan> (Accessed date: 4 December 2025).
- [24] M. Járó, A. Tóth, Scientific identification of European metal thread manufacturing techniques of the 17–19th centuries, *Endeavour* 15 (1991) 175–184, doi:10.1016/0160-9327(91)90124-T.
- [25] A. Karatzani, The use of metal threads in the decoration of late and Post-Byzantine embroidered church textiles and post-Byzantine embroidered church textiles, (2021). <https://doi.org/10.4000/ceb.18830>.